



# Effect of Exhausted Olive Cake Contamination on Fly and Bottom Ash in Power Plants

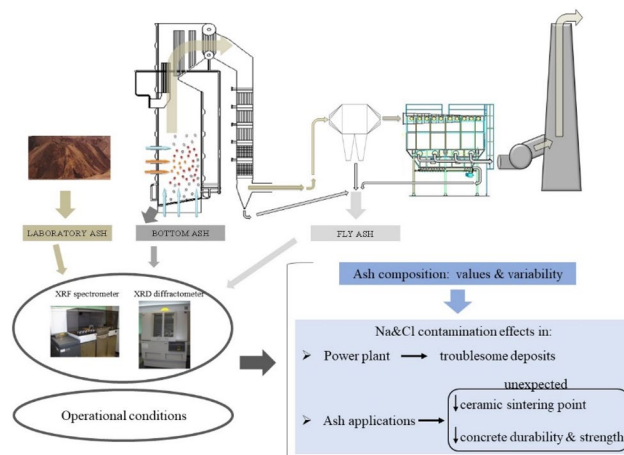
Amparo Pazo<sup>1</sup> · Magín Lapuerta<sup>2</sup> · Anselmo Acosta<sup>3</sup> · Juan J. Hernández<sup>2</sup> · Esperanza Monedero<sup>1</sup>

Received: 21 May 2021 / Accepted: 6 October 2021 / Published online: 25 October 2021  
© The Author(s) 2021

## Abstract

With the aim to prevent possible power plant malfunction due to the feedstock properties and suggest possible ash applications, feedstock samples and bottom and fly ash samples collected along more than a year in a 16 MW suspension-fired boiler power plant, fed mainly with pulverized exhausted olive cake (orujillo), were studied. A detailed characterization of fly and bottom ash has been done, as well as a seasonal evolution study. Altogether in order to find any trend on the ash composition changes and to study the relationship between ash (both fly and bottom fractions) and, on the one hand, the feedstock composition, and on the other hand, the troublesome deposit formation. A relationship between deposit growth and higher Cl and Na content in the feedstock has been noticed, showing the need for some control on these feedstock's components. The high Cl and Na content is attributed to external contamination. Furthermore, the high Al content in the feedstock and the strong relationship between Al, Fe and Si (indicating a common origin) suggest some biomass soil contamination. However, no relationship was observed between troublesome deposit formation and the hypothesized biomass soil contamination.

## Graphic Abstract



**Keywords** Biomass · Power plant · Fly ash · Bottom ash · Exhausted olive cake · Orujillo

## Statement of Novelty

Biomass residues from olive oil industries are becoming a valuable source of renewable energy. This study contributes to increase the knowledge on the effect of biomass composition on the formation of troublesome deposits and the possible sources of seasonal or accidental contamination. This

✉ Magín Lapuerta  
Magin.Lapuerta@uclm.es

Extended author information available on the last page of the article

knowledge may benefit the management of power plants, helping find the optimal operational parameters, defining the biomass components which should be carefully controlled, and providing the appropriate ash characteristics for their industrial valorization.

## Introduction

A very essential requirement to control the deposit growth in biomass boilers is to know the characteristics of the biomass ash forming matter and of the different ash fractions: bottom ash, fly ash collected in the gas cleaning system (fly ash in our study) and fine fly ash escaping by the stack (dust in this paper) generated at a specific boiler. The characteristics and quantity of the ash fractions are dependent on the ash-forming matter from the feed biomass and on the boiler type and operational conditions. Several studies have been conducted on this topic. Bashir et al. [1] showed how straw fly ash differs according to the boiler (grate or suspension one). They found that fly ash from straw suspension firing contains high contents of Si, K and Ca, while fly ash from straw grate firing is rich in the volatile elements K, Cl and S [1]. This is mainly because in grate boilers the relative importance of finest particles (composed mainly of K, S, Cl) in fly ash is high, whereas in suspension boilers the importance of this fraction is lower due to the large amount of ash matter dragged by the flue gas, and finally enclosed in the fly ash (the percentage of fly ash in suspension boilers is around 75–80% in front of the percentage in grate boilers < 20% [2]). However, regardless the boiler or biomass employed, an enrichment in volatile species in fly ash (K, Cl, S [1–5], Zn, Pb, Cd [3, 6]) and a depletion in bottom ash [3, 4] are often shown with respect to the original ash forming matter. Such enrichment is even higher in grate boilers. Nevertheless, a slight depletion of K in fly ash of pure straw, burned in suspension boiler conditions was detected by Nordgren et al. [7]. Fly ash volatile enrichment depends on the amount of volatile compounds in the biomass, on their previous devolatilization, on the subsequent homogeneous and heterogeneous condensation, on the amount of non-volatile species dragged by the gas and on the efficient retention of finest particles by the ash recovery systems. These factors are strongly related to the kind of boiler and operational conditions (which affect the contact likelihood between solid and gaseous phases (strongly dependent on boiler type [7]), the % of fly ash, exit temperatures, filtering efficiency...) and also on biomass properties.

A strategic energy source in Europe, and especially in the southwest European Mediterranean areas, is exhausted olive cake (orujillo). Its high heating value (lower heating

value between 14 and 17.5 MJ/kg ar -as received-) and its low moisture (it is usually marketed with moistures between 9 and 16% ar) make it a feasible fuel to be used as unique or main fuel, which is a significant practice in these areas. The main applications are medium-sized boilers to generate steam for on-site thermal use at olive oil industries and also power plants with or without steam cogeneration (in Andalusia, Spain, plants with power generation only, ranging from 8 to 16 MWe [8]). Furthermore, it has been used in co-firing in large coal plants in Europe [9–11] because of its easy grinding, which allows its incorporation in coal pretreatment systems with minimal modifications [11], and because of its easy feeding, with no flowing problems given its granular shape and particle size (mostly below 8 mm). Despite coal firing is disappearing in the EU and in UK due their climatic impact, much of the rest of the World has energy programs that still depend on coal for the near future, and orujillo could be a good renewable co-fuel to be used.

Orujillo is composed of de-oiled peel, pulp and kernels from olive fruit. It is the final residue/by-product produced in olive oil extraction. It is a de-oiled and dried solid residue obtained after extraction with solvents of the residual olive oil from the olive cake, which is a residue of the olive oil mechanical extraction process. A remarkable characteristic is its high potassium and chlorine content (K = 1.75% and Cl = 0.1–0.4% dry basis [12]) which have great influence on fouling [13–16] and corrosion [15, 17] processes. Therefore, boiler conditions should be carefully defined in order to avoid uncontrolled deposit growth and malfunctions. However, power plants using this feedstock are prepared for it. Problems arise when orujillo with higher content of harmful elements is used. Orujillo with higher content in chlorine and sodium derived from external contamination (for example, an eventual source of NaCl contamination is the exposition to sea water or road salting [12, 18]), or specific treatments used in olives being dressed with salt (NaCl solution) or soda (NaOH solution, i.e. lye) for table olives [19, 20] could occasionally arrive. When this occurs, serious problems of uncontrolled deposit growth often arise in the boilers [21].

Limited data on recovery ash is available from large scale biomass suspension boilers [1, 2, 5, 22–25] and it is mainly focused on fly ash. Since contamination of biomass, either accidental or seasonal, may occur, the major objective of this study is to present detailed characterization of fly and bottom ash obtained during more than a year campaign in a suspension boiler, in order to find any trend on the ash composition changes. This requires studying the relationship between recovery ash (both fly and bottom fractions) and composition of biomass ash, and finding correlations between the elements composing

both of them as well as seasonal patterns. This knowledge has two benefits: a) to prevent boilers from biomass that could eventually cause harmful deposit formation (in fact deposit formation associated with contamination has been detected in the analyzed period) and b) to find possible applications for the fly and bottom ash. Moreover, although neither the ash content nor the composition of the feedstock are usually considered in the fuel quality control procedure implemented in power plants because of their high cost [26], the results of this work could be useful to determine which ash components should be measured periodically (maybe in external labs), at least when changing the fuel supplier or the fuel origin.

## Experimental

### Power Plant

Biomass and combustion residues (fly and bottom ash) were sampled from a 16 MW suspension-fired boiler power plant (Energías de la Mancha, S.A) located in Villarta de San Juan, Spain. The fuel employed during the study was a mixture of:  $\geq 95$  % wt. of exhausted olive cake (orujillo) and  $\leq 5$  % wt. of other pulverized biomass (wood, exhausted grape cake, almond shell and others). Table 1 summarizes the plant operational characteristics,

including the main fuel characteristics: kind of fuels, particle size and usual moisture. Figure 1 presents a scheme of the boiler and ash recovery system. Around 80% of the fly ash was collected at the bag filter, 15% at the multicyclone and 5% at the boiler final collector.

### Sampling

A combined sample for biomass, for fly ash and for bottom ash were taken once a month during 15 months, plus 8 fly ash samples during 8 additional months. To get a representative sample, the biomass combined sample was composed of increments of all the biomass consumed during a period of time (about one day) and the corresponding fly and bottom ash increments were taken assuring that they came from the combustion of this biomass. Depending on the sampling time, every combined sample consisted of 8 to 11 increments. For the different kinds of samples, the sampling plan was:

- The biomass increments were taken at the burner's feed hoppers during the filling up process of the ash storage silo according to the scheme shown in Fig. 2. Sampling started with an empty ash storage silo and finished one hour before the new silo discharge to ensure the concordance between biomass and fly ash sampled.
- Bottom ash increments were taken at the bottom ash discharge following the same biomass scheme (Fig. 2).

**Table 1** Main plant and operational characteristics

	Normal operation
Unit capacity	55 MW <sub>th</sub>
Electric capacity	16 MW
Usual gross electric output	14–14.5 MW
Usual steam production	61–62 tons/h
Total air flow rate	60–66 tons/h
Superheater steam temperatures	280–450 °C
Flue gas temperatures at superheater inlet	650–700 °C
Flue gas temperatures at boiler generator bank outlet	390–420 °C
Soot blowing (of dry steam) frequency	3–6 times per 8 h
Fuel	Primary: Orujillo $\geq 95$ wt. % Secondary: wood, forest chips, exhausted grape cake, almond shell etc. $\leq 5$ wt.
Feed biomass particle size	$\leq 1.2$ mm
Feed biomass moisture	12–17 wt. % (wet basis)
Usual biomass consumption	12.5 tons/h (wet basis)
Biomass consumption per year <sup>a</sup>	$91.2 \times 10^3$ tons/year (wet basis)
Fly ash production per year <sup>a</sup>	$6.3 \times 10^3$ tons/year (wet basis)
Bottom ash production per year <sup>a</sup>	$2.5 \times 10^3$ tons/year (wet basis)

<sup>a</sup>Mean values during the fifteen-month period study

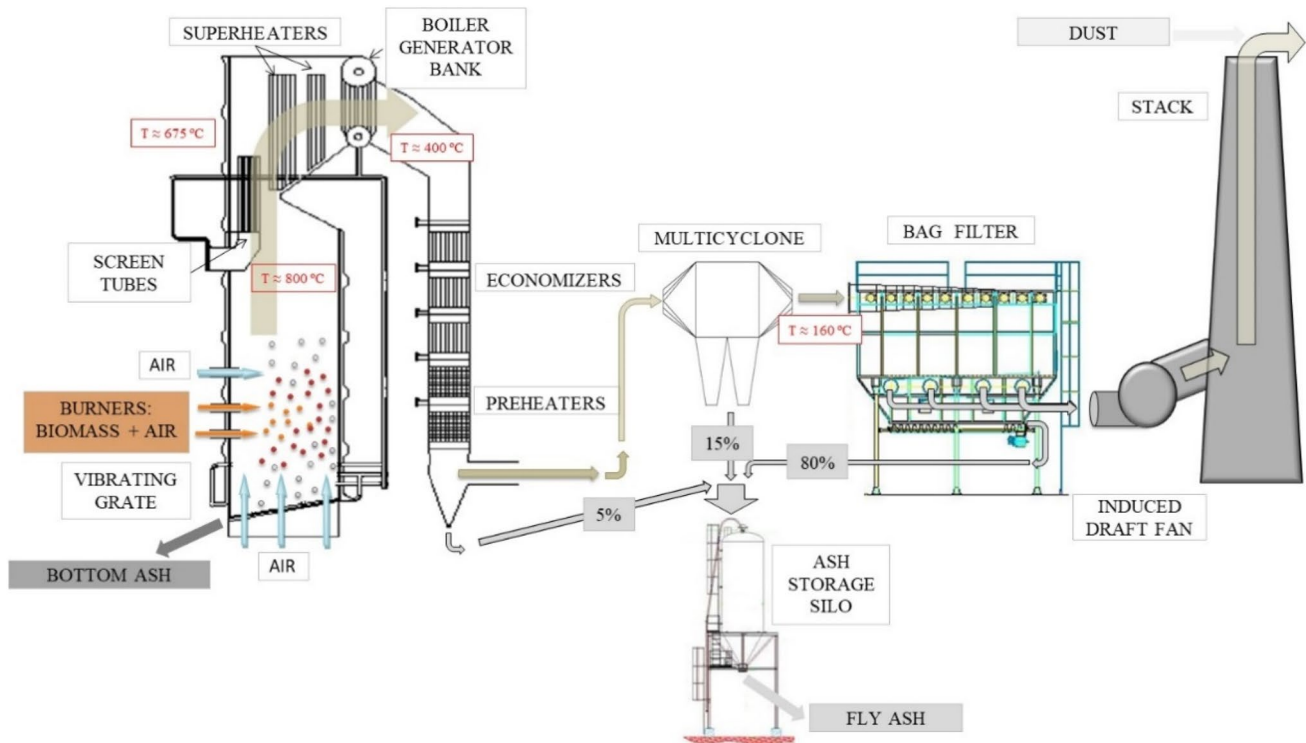


**Fig. 1** Schematic view of the boiler and ash recovery systems during the study. Percentage numbers indicate the average contribution of the different parts of the recovery system to the fly ash

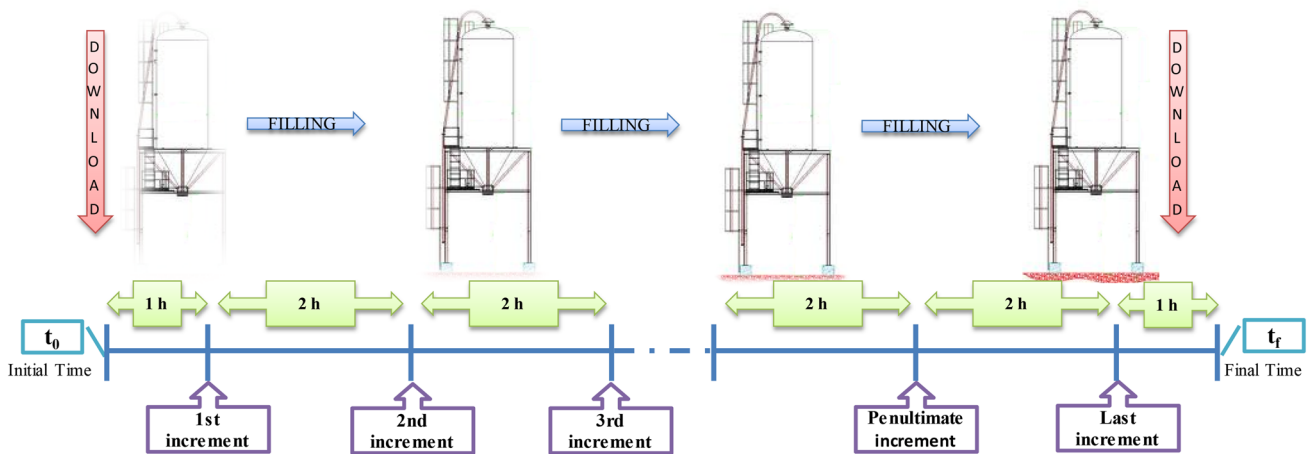


**Fig. 2** Scheme for the collection of increments of biomass and bottom ash samples

Bottom ash was incandescent at the sampling point. It is composed of two fractions, fine and coarse, and only coarse fraction was taken. The coarse fraction represents 75% of total bottom ash.

- Fly ash increments were taken at constant time intervals during the discharge of ash from the storage silo. Fly ash temperature at the collecting point was room temperature.

The total time for sampling was not always the same because it was dependent on the arrival time of the truck transporting fly ash, which is variable.

### Test and Laboratory Equipment

Table 2 summarizes the methods and the equipment used to analyze biomass and combustion residues (bottom and fly

**Table 2** Summary of methods and equipment for characterization

	Standard	Method	Equipment
<i>Biomass</i>			
Proximate analysis			
Volatiles	EN 15148	Air contactless heating at 900 °C	Muffle furnace
Ash	EN 14775	Air heating under controlled heating ramps up to 550 °C	Muffle furnace
Ultimate analysis			
C, H, N / S	EN 15104 / EN 15289	High oxygen combustion—Gas analysis: -C,H,S infrared absorption -N thermal conductivity	Elemental analyzer (LECO—TruSpec)
Cl	EN 15289	Biomass microwave acid digestion—Liquid Ion chromatography analysis	Microwave—Ion chromatograph (883 compact IC Pro, Metrohm)
O	EN 15296	By difference, including ash content	–
<i>Ash samples: biomass ash (laboratory ash<sup>a</sup>) and combustion residues (fly and bottom ash)</i>			
Chemical composition (expressed as oxides except for Cl): Al, Ca, Fe, K, Mg, Na, P, Si, Cl, S	–	X-ray fluorescence (XRF)	X-ray fluorescence spectrometer (Magix Pro, Panalytical)
Crystalline phases	–	X-ray diffraction (XRD)	X-ray diffractometer (X'Pert MPC, Panalytical)

<sup>a</sup> Biomass laboratory ash made at 550 °C

ash). Below some of the analysis are described with more detail.

Ash chemical composition was determined with semi-quantitative X-ray fluorescence technique (XRF), on powdered sample. Loss on ignition (LOI) was determined by heating ash powders (from all types of ash: fly, bottom and laboratory) in a muffle furnace at 1100 °C for 5 h. Laboratory ash samples were produced from the biomass samples to determine their chemical composition. Standard EN 14,775 was followed with a final temperature of 550 °C.

The crystalline phases were detected in the ash with a powered X-ray diffractometer (X'Pert MPC, Panalytical) using Cu K<sub>α1</sub> radiation. The scan was run from 3° to 75° (2-theta-scale), with increments of 0.05° and a counting time of 0.5 s per step. Identification of compounds was made using the Joint Committee on Powder Diffraction Standards (JCPDS) database. Diffractograms obtained are complex multicomponent systems with too many peaks in which different compounds can be overlapped. Therefore, for a better determination of the crystalline phases, the samples were water washed to separate water-soluble phases (such as chlorides, sulfates, and some carbonates) from other insoluble phases (such as quartz, silicates and some phosphates) which remain in the solid residue. Then, comparing diffractograms of the original sample from that of the insoluble fraction, it is easier to identify the peaks from soluble phases, since they are not present anymore in the latter diffractogram.

## Statistical Analysis

The statistical analysis was performed by using Statistical Package for Social Sciences (SPSS version 24) using hierarchical cluster analysis. Clustering techniques involve measurement of the distances (differences) and the resemblances between the samples to be clustered. The samples are grouped in clusters according to their similarity. In this work, similar groups of monthly ash samples composition were searched considering the following compounds: SiO<sub>2</sub>, Al<sub>2</sub>O<sub>3</sub>, Fe<sub>2</sub>O<sub>3</sub>, MgO, CaO, Na<sub>2</sub>O, K<sub>2</sub>O, P<sub>2</sub>O<sub>5</sub>, SO<sub>3</sub> and Cl. The results were standardized using the Ward Grouping Method with Square Euclidean Distance as show in Eq. 1 where *a* and *b* are two different samples. The results were analysed from their respective dendograms.

$$\|a - b\|_2^2 = \sum_i^n (a_i - b_i)^2 \quad (1)$$

Since only fly ash samples were taken for all the period studied, the hierarchical cluster analysis were performed only with this type of samples.

Moreover, coefficient of variation (*C<sub>v</sub>*), defined as the ratio of the standard deviation (*σ*) to the mean value (*μ*, Eq. 2), was used to express the variability of the different properties at the biomass and ash collected in different months. The higher *C<sub>v</sub>*, the higher heterogeneity of the variable.

$$C_v = \frac{\sigma}{|\mu|} \times 100 \quad (2)$$

## Results and Discussion

### Feedstock and Recovery Ash Composition: Values and Variability

#### Chemical Composition

Thermochemical properties and proximate and ultimate analysis of the feed biomass consumed during the 15 months are summarized in Table 3 and the chemical composition of biomass ash (concentrating the inorganic components of the biomass) is shown in Fig. 3 (this data, together with TiO<sub>2</sub> and MnO, which are not shown in the figure due their low value (<0.5%), are included as a table in the Supplementary Material). Unfortunately, when the samples taken in December (1st year) and August (2nd year) were inspected, they were rotted, so there are no results from these samples. Values obtained show that C, H, N, S, volatile matter, and calorific value obtained in all the tests are quite constant over time (their respectively coefficients of variation ( $C_v$ ) are less than 10%), while Cl and ash content are more variable, particularly chlorine content which has an extremely high coefficient of variation, 41%. The average ash content at 550 °C (11.11% wt.) is close to the maximum of the typical range shown in the literature for exhausted olive cake [12], the main component of biomass samples in this plant ( $\geq 95\%$ ). Mean contents of carbon, hydrogen, nitrogen, sulfur, chlorine and oxygen are within the typical range for orujillo. However, the sample from November (1st year) has an extremely high concentration of chlorine (Table 3) and sodium (shown through the biomass ash composition in Fig. 3), more than expected for orujillo and the other biomass used in the feed mixture [12], and 2.5 and 18.2 times higher, respectively, than the average content of these elements without considering this month. This extremely high Cl and Na content also occurs during December (1st year) and was reflected on the fly ash composition (Fig. 4). The unusual high chloride and sodium content should be related to an orujillo contamination, which could derive from different causes. For example, the infrequent employment of table olives dressed with sodium chloride and, in some cases, with lye, in the olive oil production process. The process to obtain table olives from fresh olives increases the Cl and Na contents. For instance, Na content of olive pulp and peel varies from around 10–40 ppm of fresh olive [27] to 5700–16,600 ppm for table olives (value variable depending on origin and treatment) [20]. Spanish standard [28] prevents from the thermal use of fuels derived from

table olives. Other eventual source of Na and Cl contamination are the exposition to sea water or road salting [12, 18] or other non-controlled contaminations.

This period of unusually high Cl and Na content (November (1st year) and December (1st year)) led to an uncontrolled superheater deposit growth and to a complete flue gas blockage and plant shutdown in December 1st year. As reported in the literature, chlorine and alkaline elements are the main elements affecting fouling deposit formation [1, 13, 15]. Furthermore, it was proved that Na causes the molten state of deposit structures, which increases the capturing efficiency and the tenacity of the deposits, leading to large deposits, difficult to be removed [21]. Therefore, it is necessary to include the control of Cl and Na content in the plant feedstock's quality control. Traditionally, power plants control fuel moisture [26] and, some of them, heating value. However, these measurements cannot alert from high Cl and Na contents.

Figure 4 and 5 show fly and bottom ash compositions respectively for all the samples collected (numerical data included as a table in the Supplementary Material). As expected, the composition variability of the recovery ash is high but it is clear that the main oxide, when results are expressed as oxides, is K<sub>2</sub>O for both, fly ash (39.35% wt. in average) and bottom ash (27.88% wt. in average). However, SiO<sub>2</sub> (20.07% wt. in average) and CaO (17.92% wt. in average) are also high in bottom ash.

For fly ash the coefficient of variation of the different compounds is around 20–35% except for potassium (K<sub>2</sub>O), that remains almost constant (coefficient of variation 5.8%), sulfur and phosphorous (8.8 and 9.7% respectively), and sodium, with an extremely high variation (coefficient of variation 118%). The high sodium's coefficient of variation is mainly due to the extremely high content in November (1st year) and December (1st year), that constitute an unusual composition with respect to the results from all other months, in agreement with the composition of feedstock ash (laboratory ash). Excluding these months, all coefficients of variation decrease, but this decrease is considerably higher for sodium (which drops to 57%, half of the initial one) and chlorine (which drops to 6.2%, being 22.6% the initial one). Differentiation from November and December (1st year) with respect other months is confirmed by the statistical analysis carried out using clustering techniques. As can be seen in Fig. 6, the smallest and most homogeneous group, when analyzing simultaneously all chemical compounds, was observed for November (1st year) and December (1st year) samples. Furthermore, the separation between groups shows a high linkage distance between the November–December 1st group from the group formed by the other samples. This linkage distance is similar to that observed by Zajac et al. [29] between different kinds of biomass. Therefore, separation between

**Table 3** Thermochemical properties and proximate and ultimate analysis of biomass samples (dry basis)

Month	Year	Proximate analysis			Ultimate analysis						Heating value		
		Volatile matter (VM)	Ash (A)	Weight %	C	H	N	S	Cl	O	High Heating Value (HHV)	Low Heating Value (LHV)	MI/kg
November	1st	70.66	8.59		49.40	6.27	1.50	0.12	0.56	33.56	20.90	19.54	
December <sup>a</sup>	1st	–	–		–	–	–	–	–	–	–	–	
January	1st	70.64	9.10		50.39	5.81	1.56	0.11	0.24	32.79	20.17	18.91	
February	1st	70.49	10.10		49.55	5.51	1.64	0.10	0.26	32.84	19.50	18.31	
March	2nd	69.80	12.83		48.29	5.71	1.55	0.11	0.18	31.33	19.28	18.11	
April	2nd	69.89	11.37		48.69	5.69	1.90	0.12	0.33	31.90	19.41	18.25	
May	2nd	69.70	12.44		48.03	5.68	1.59	0.13	0.25	31.88	19.35	18.20	
June	2nd	69.46	12.16		48.18	5.63	1.48	0.12	0.23	32.20	19.36	18.20	
July	2nd	70.08	11.27		48.94	5.73	1.61	0.13	0.23	32.09	19.70	18.52	
August <sup>a</sup>	2nd	–	–		–	–	–	–	–	–	–	–	
September	2nd	71.22	9.93		49.00	5.95	1.62	0.13	0.20	33.17	20.28	18.99	
October	2nd	68.73	12.23		48.58	5.83	1.67	0.14	0.23	31.32	20.11	18.85	
November	2nd	68.99	12.29		48.15	5.84	1.61	0.14	0.21	31.76	19.93	18.67	
December	2nd	66.37	12.15		48.99	5.55	1.67	0.13	0.17	31.34	19.90	18.70	
January	2nd	69.73	9.91		48.39	5.82	1.48	0.13	0.16	34.11	19.62	18.36	
Minimum		66.37	8.59		48.03	5.51	1.48	0.10	0.16	31.32	19.28	18.11	
Mean		69.67	11.11		48.81	5.77	1.61	0.12	0.25	32.33	19.81	18.58	
Maximum		71.22	12.83		50.39	6.27	1.90	0.14	0.56	34.11	20.90	19.54	
Average deviation		0.79	1.22		0.52	0.14	0.07	0.01	0.06	0.74	0.37	0.33	
Sample standard deviation		1.21	1.41		0.67	0.19	0.11	0.01	0.10	0.90	0.47	0.41	
Coefficient of variation (%)		1.7	12.7		1.4	3.4	6.8	8.8	41.4	2.8	2.4	2.2	
Typical values for exhausted olive cake (EN ISO 17225–1 [12])		–	3.4 – 11.3		48–52	4.6–6.3	1.4–2.7	0 – 0.5	0.1 – 0.4	33	18.1 – 21.6	13.9 – 19.2	

<sup>a</sup>Corrupted and not analyzed

**Fig. 3** Laboratory ash chemical composition

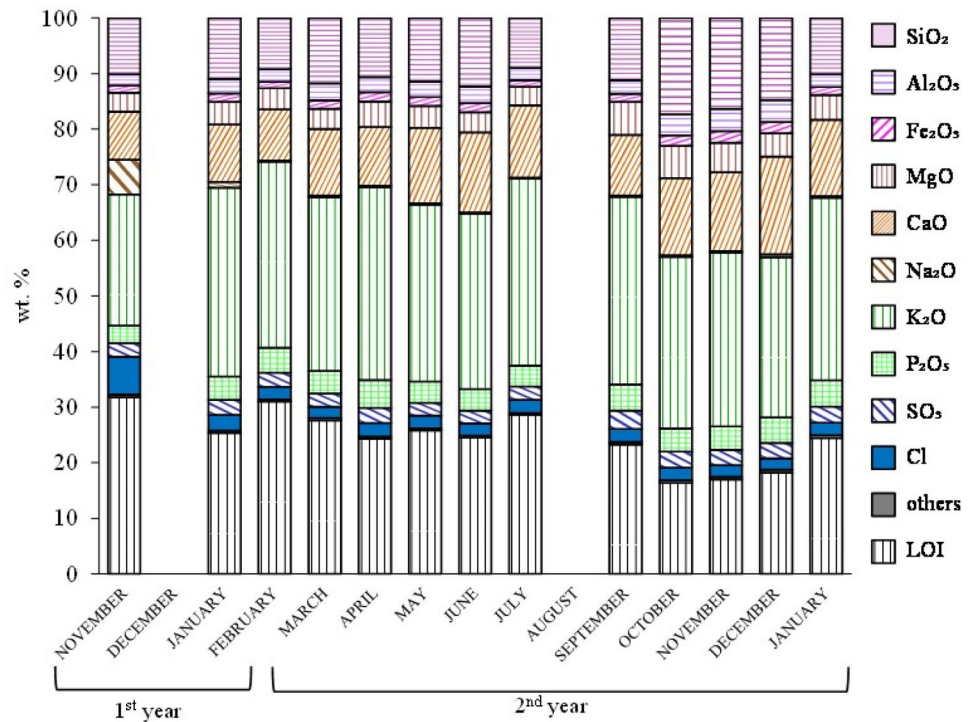
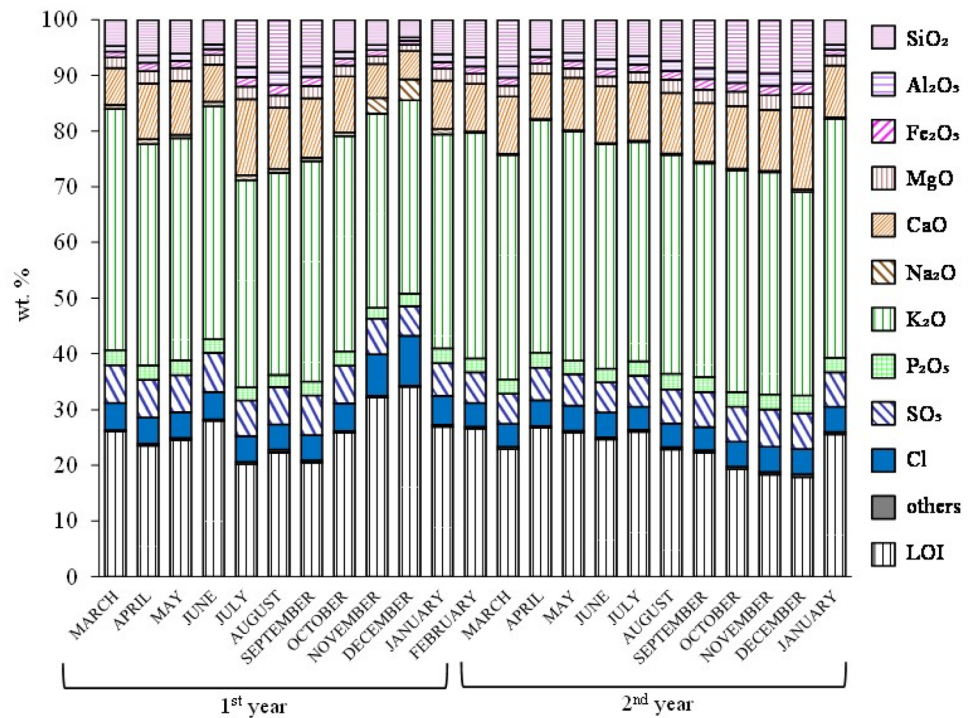


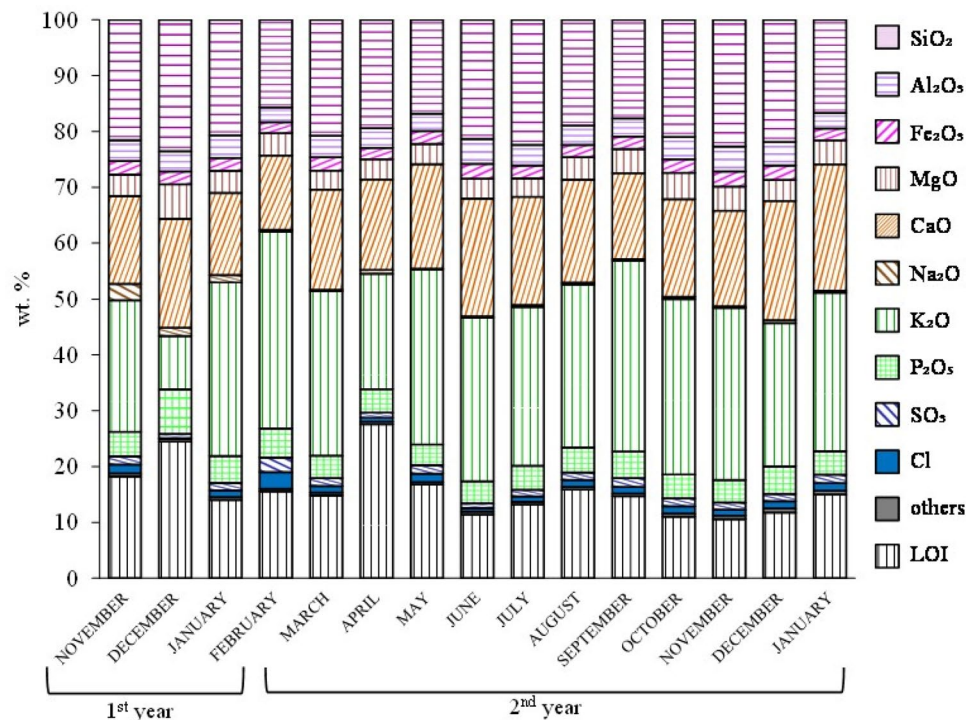
**Fig. 4** Fly ash composition



groups seems to confirm the unusual Cl and Na contents at these months. This high Na content, together with the high chlorine content, led to harmful deposit formation, due to the major role that high alkaline and chlorine contents play in the deposition process [1, 4, 30].

For bottom ash the coefficient of variation of the different compounds is around 10–30%. The least variable oxide content is that of  $\text{Fe}_2\text{O}_3$  (coefficient of variation 9.8%) whereas the most variable one is the  $\text{Na}_2\text{O}$  content (coefficient of variation 111.8%), accordingly with fly ash



**Fig. 5** Bottom ash composition

results. Likewise, the variability decreases when excluding the months with an unusual composition (November (1st year) and December (1st year)).

Figure 7 shows the average composition of laboratory, fly and bottom ash considering all samples except November (1st year) and December (1st year) due to their unusual composition. The main components in laboratory ash are K<sub>2</sub>O (32.32% wt.), CaO (12.78% wt.) and SiO<sub>2</sub> (12.08% wt.). Similarly, the main component, in fly ash is K<sub>2</sub>O (39.96% wt.), four times higher than the second one (CaO (10.23% wt.)). Contents in SiO<sub>2</sub> (7.31% wt.), SO<sub>3</sub> (5.91% wt.) and Cl (4.47% wt.) are also important. For bottom ash, K<sub>2</sub>O (29.66% wt.) is also the main component, but SiO<sub>2</sub> (19.75% wt.) and CaO (17.93% wt.) contents are also high, whereas SO<sub>3</sub> (1.41% wt.) and chlorine (1.28% wt.) are less abundant (data included in the Supplementary Material). Furthermore, Fig. 7 shows how the orujillo ash forming matter (denoted as laboratory ash) is distributed among the ash fractions (fly and bottom). As shown, the enrichment in volatile elements (K, S and Cl, expressed as oxides in the figure) in fly ash and the enrichment in Si, Al, Fe, Ca and P in bottom ash with respect to the laboratory composition can be clearly observed. The higher K, S and Cl contents in fly ash are due to the vaporization of these elements, their reactions, and the subsequent condensation of the formed species containing these elements, on already existing ash particles or nucleation of new particles. These results are consistent with other combustion biomass studies [1–5]. Nevertheless, the fly ash from orujillo shows

higher potassium content than fly ash from straw (biomass also with high K and Cl contents) as shown in other studies, despite different analysis techniques [1]. This could be explained not only by the initial high potassium content of orujillo but also by the better release of potassium, at pulverized combustion conditions, for olive residue than for straw, as shown by Shah et al. [31].

According to their composition, all ash samples are classified as low acid “K” type following the chemical classification system of inorganic matter in biomass and biomass ash proposed by Vassilev et al. [18] (Fig. 8). This classification is also used by Eliche-Quesada and Leite-Costa [25] for the same kind of ash, although in their article they misclassify their sample as “C” type. Categorization of ash type is useful when looking for possible applications. These applications are discussed in the last section (Ash Applications).

### Phase Composition

The study of phase minerals identified by XRD shows some general conclusions. A broad halo can be observed from the XRD patterns, which is associated with presence of a large amount of amorphous materials. There are some phases which have been identified in all months, while other phases could only be identified in certain months. Table 4 summarizes the identified crystalline phases for each kind of ash, and distinguishes those which have been identified for all samples from those which have been identified in most samples but not all. As a representative example, diffractograms

**Fig. 6** Dendrogram with the groups division of fly ash based on chemical composition

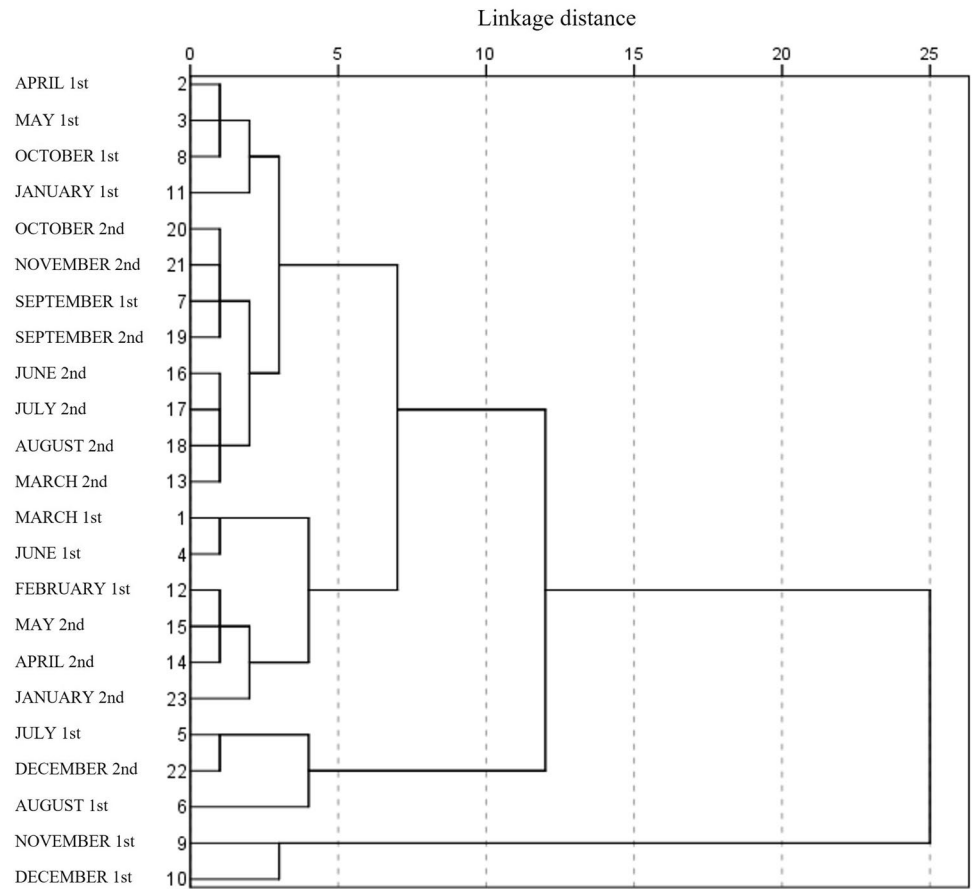


**Fig. 7** Average composition values of laboratory, fly and bottom ash (discarding the abnormal November and December 1st year months)

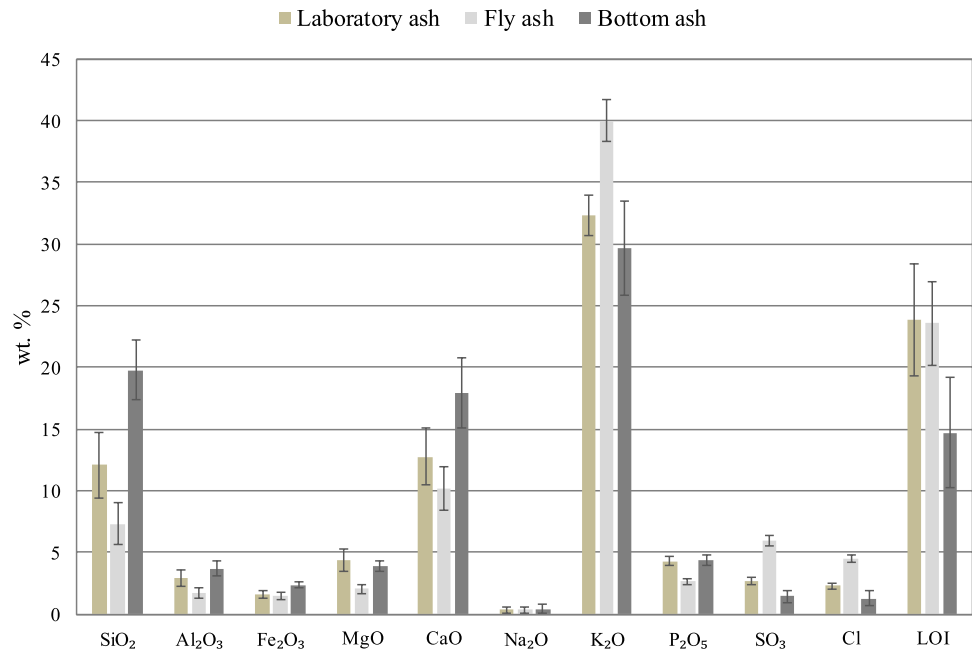
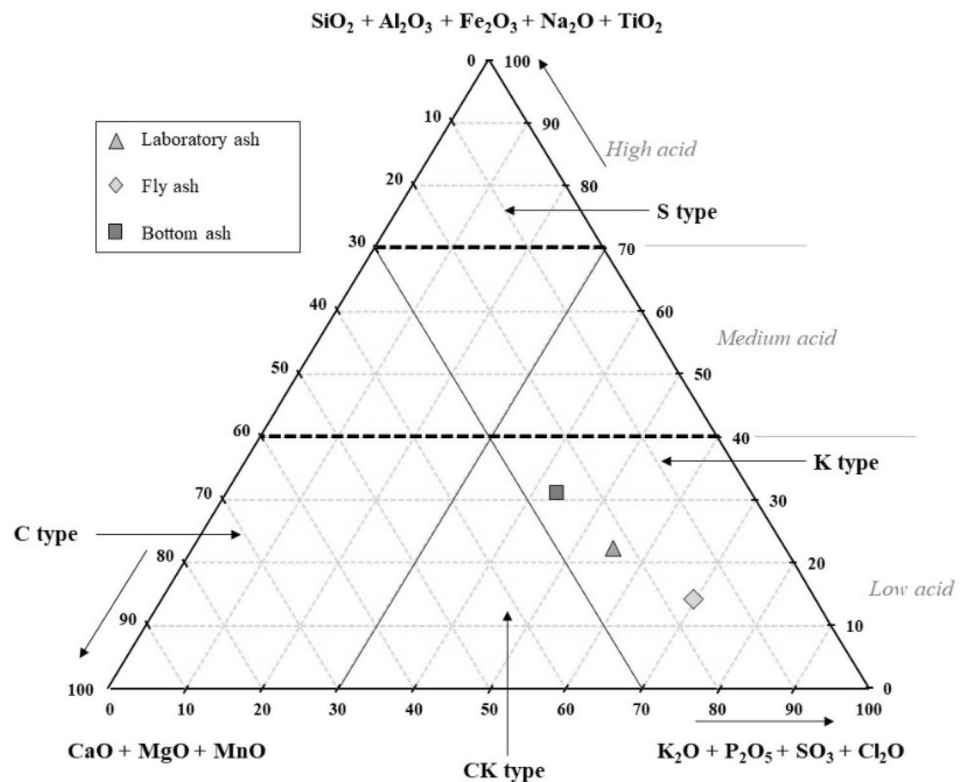


**Fig. 8** Position of the average ash composition in the chemical classification system of inorganic matter in biomass and biomass ash from Vassilev et al. [18]



showing XRD results are shown in Figs. 9, 10, 11, and the peaks of the identified crystalline phases are marked with the acronyms shown in Table 4. As an example and for a better visual comparison, the diffractograms of all kinds of ash for a particular month and, their water insoluble fraction, are shown in a single figure (Fig. 12). In these figures (from 9 to 12), the halo associated with amorphous material can be observed, and it is remarkable at the moving range of  $25^\circ\text{--}35^\circ$  ( $2\theta$  for Cu  $K_{\alpha 1}$  radiation). The relative importance of the different identified phases clearly changes along the different months. For example, at laboratory ash (Fig. 9), Fairchildite is the peak of maximum intensity at June 2nd whereas Quartz is the most intense peak at November 2nd. As shown in Table 4, most of the phases identified are common in the different kinds of ash, although with different relative intensity. Sulphates and chlorides are more intense in laboratory ash and, especially, in fly ash, while silicates and phosphates are intense in bottom ash (Figs. 9, 10, 11). Carbonates are also identified in all kinds of ash. These results are consistent with their classification as “K type” ash, and with the results from XRF (for example, higher S and Cl content in fly ash).

Laboratory ash is useful as a reference to compare with industrial ash. However, the high temperature and short residence time of biomass in a suspension-fired boiler affect the amount of volatile matter present in the bottom and fly ash (some of this volatile matter, such as alkaline salts,

governing fouling) and the crystalline phase transformations. Although the analysis of laboratory ash is useful to prevent from possible problems, since it warns from the presence of harmful elements and compounds, it does not provide information about the specific composition of the real ash at the deposit locations (grate, superheaters, etc.).

The main carbonates found are potassium and calcium carbonates (Table 4). Calcite has been identified in all laboratory samples, although it is not always marked in Fig. 9 for clarity. The same applies to most of the bottom and fly ash samples. Fairchildite is specific of laboratory ash and huntite appears in both fly and bottom ash, especially in the latter. In bottom ash, the carbonates of calcium and magnesium are more significant than the potassium ones.

Quartz ( $\text{SiO}_2$ ) has been identified in all ash samples (Table 4). Other silicates, such as potassium aluminosilicates ( $\text{KAlSi}_4$ ) are found in all bottom and fly ash. However, in fly ash, this phase is masked by a high water-soluble peak. Although under more aggressive conditions it could be solubilized, in this case it is better identified in the insoluble fraction (Fig. 12 peak at  $2\theta = 28.50^\circ$ ). A specific silicate, talc, is only identified in the insoluble fraction of the laboratory ash (Fig. 12 peak at  $2\theta = 28.60^\circ$  and  $2\theta = 9.47^\circ$ , the last not shown), although it cannot be observed in the original ash. Talc is not a usual phase in biomass ash, but it is a common additive used to improve oil extraction which finally

**Table 4** Crystalline phases identified. (●) Identified in all ash samples (○) Identified in most of ash samples but not all

Crystalline phase			Ash		
Phase name	Acronym	Chemical formula	Laboratory	Fly	Bottom
Chlorides					
Sylvite	Sy	KCl	●	●	○
Halite	Ha	NaCl	○ <sup>(a)</sup>	○ <sup>(a)</sup>	
Silicates					
Potassium aluminium silicate	Ks	KAlSiO <sub>4</sub>		●	●
Potassium magnesium silicate	KMg	K <sub>2</sub> MgSiO <sub>4</sub>			○
Talc	T	Mg <sub>3</sub> Si <sub>4</sub> O <sub>10</sub> (OH) <sub>2</sub>	●		
Quartz	Q	SiO <sub>2</sub>	●	●	●
Carbonates & bicarbonates					
Potassium carbonate	Kc	K <sub>2</sub> CO <sub>3</sub>	○	○	
Potassium carbonate hydrated	Kh	K <sub>2</sub> CO <sub>3</sub> (H <sub>2</sub> O)1.5	○	○	
Kalicinite	K	KHCO <sub>3</sub>	○		○
Fairchildite	F	K <sub>2</sub> Ca(CO <sub>3</sub> ) <sub>2</sub>	○ <sup>(b)</sup>		
Huntite	H	CaMg <sub>3</sub> (CO <sub>3</sub> ) <sub>4</sub>		○	○
Calcite	Cc	CaCO <sub>3</sub>	●	○	○
Phosphates					
Chloroapatite	ApCl	Ca <sub>5</sub> (PO <sub>4</sub> ) <sub>3</sub> Cl <sub>0.9</sub> F <sub>0.1</sub> Ca <sub>5</sub> (PO <sub>4</sub> ) <sub>3</sub> Cl		●	○
Hydroxylapatite	ApH	Ca <sub>10</sub> (PO <sub>4</sub> ) <sub>6</sub> (OH) <sub>2</sub>		●	○ <sup>(c)</sup>
Potassium phosphate	P	K <sub>4</sub> P <sub>2</sub> O <sub>7</sub>			○
Sulphates					
Arcanite	Arc	K <sub>2</sub> SO <sub>4</sub>	●	●	

<sup>(a)</sup>Halite is identified in November and December 1st

<sup>(b)</sup>Fairchildite is identified in all laboratory ash samples except November 1st

<sup>(c)</sup>Hydroxylapatite is identified in all bottom ash samples except December 1st and April 2nd

ends up at the olive cake [32]. It is usually added in a range of 0.5% to 2% of the olive weight.

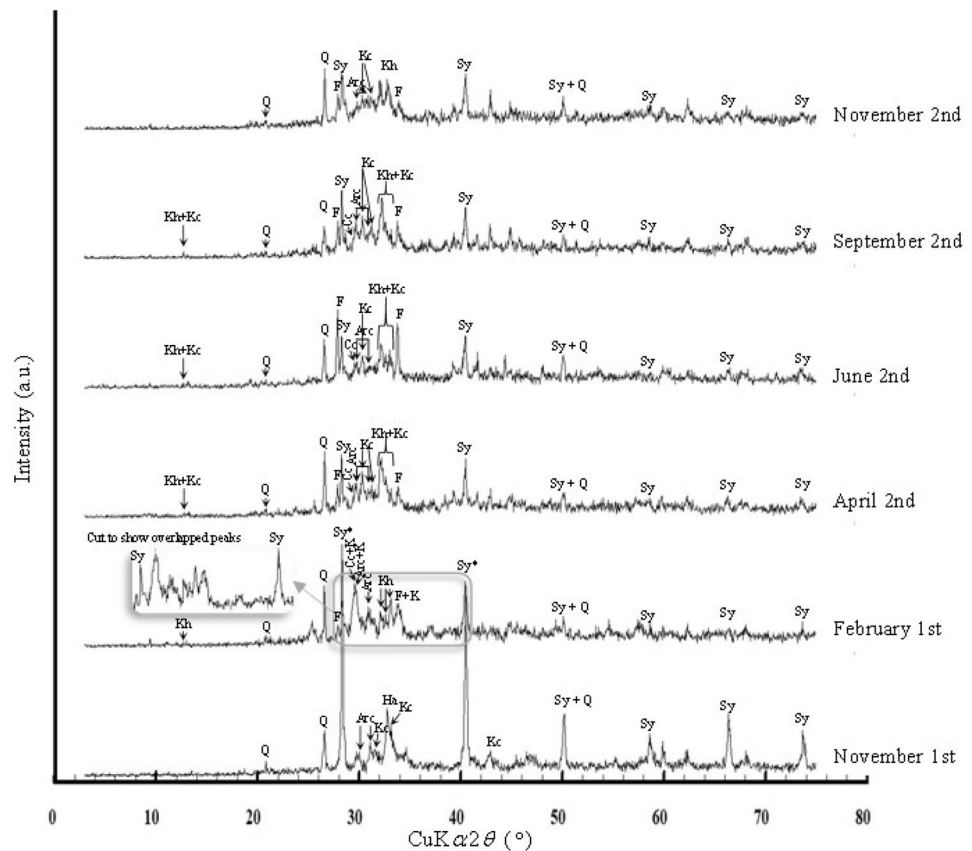
Phosphates in the form of apatites (chloro- and hydroxyl-) are the most repeatedly found. They are present in fly and bottom ash (Figs. 10, 11, 12, where the range of most intense peaks is  $2\theta = 31^\circ\text{--}34^\circ$ ), but their importance is higher in bottom ash, result which agrees with a higher content of phosphorous and calcium (Fig. 7). On the contrary, apatites do not appear in the laboratory ash (only soluble compounds appear within the range of most intense peaks for apatites), which suggest that they are not in the original biomass. According to these results apatites are supposed to be secondary phases, formed during the combustion process. This agrees with Vassilev et al. [33] who stated that the dominant origin of phosphates is secondary, as a result of the interaction of oxides, such as those of Ca, Fe, K, Mg, with phosphorous from the organic matter.

The presence of sylvite (KCl) in the orujillo ash is clear. It is always present on laboratory and fly ash (Table 4) and is the most intense phase in fly ash. XRD profile of November 1st laboratory and fly ash show a perfect pattern of sylvite (Fig. 9 and Fig. 10). Furthermore, its reduction

(or disappearance) in the diffraction intensities in bottom ash can be explained with the volatilization and silication of KCl, [34, 35] which for some samples is not complete and still appears in the bottom ash. On the other hand, KCl present in fly ash is mostly attributed to condensation of gaseous KCl (derived from K and Cl volatilization and recombination) over existing ash. KCl plays an essential role on deposit formation because it promotes the formation of the first deposit layer and acts as glue [36] for the impacting ash particles, facilitating deposit growth. The role of sylvite on deposits formed at this plant was widely studied in a previous work [21] and the presence of this phase was evident (it was the most intense phase in all deposits, and specially at the inner layers).

Arcanite (K<sub>2</sub>SO<sub>4</sub>) follows similar trend as KCl. It has been identified in laboratory and fly ash but not in bottom ash. Similarly to KCl, the origin of potassium sulfate in fly ash is mostly attributed to the condensation of this compound on the existing particles in the flue gas. At an initial stage, when exiting the combustion chamber, these particles have quite similar structural characteristics to those ending

**Fig. 9** X-ray diffractogram of laboratory ash (the peaks marked as Sy\* belong to the November 1st diffractogram)



as bottom ash. This initial similarity is, in some way, confirmed by the resemblance between the insoluble fractions of fly and bottom ash (Fig. 12). Later, some reactions take place, like carbonatation (in both types of ash) and condensation of volatile and soluble chlorides and sulfates (on fly ash). These are clearly identified in the original fly ash (Fig. 12) at  $2\theta$ :  $28.30^\circ$  and  $40.45^\circ$  for KCl and at  $2\theta$ :  $29.70^\circ$  and  $30.80^\circ$  for  $K_2SO_4$ .

Although the presence of NaCl has been observed on ash samples for November and December 1st, the most intense phase is still KCl in these samples. Chlorine has been widely considered as a promoter of alkalis release [31, 34]. Therefore, higher Cl content usually leads to higher alkali release, which is able to react with chlorine at the gaseous phase. Once at the gaseous phase, potassium remains in higher proportion than sodium, favoring the formation of KCl. Figure 13 presents the height of the highest peak associated with KCl along months for fly and laboratory ash samples. Highest peaks are associated with the abnormal months November and December 1st. The importance of KCl during the abnormal months on deposit formation has already been discussed. However, the higher Na content in fly ash contribute to the deposit growth, not only through NaCl, but also favoring the formation of molten states, as explained above.

### Seasonal Study and Elements Correlations

Chemical composition of fly ash, collected along 23 months, was analyzed with the aim to check any seasonal trend. Fly ash was selected for this study because this is the only type of ash reaching the superheaters, where most of the harmful deposit formation may occur. A possible relationship between the weather winter conditions and the high content on Na and Cl observed during the winter of the first year was suspected, and contamination with road salt treatment was presumed to be the cause. In addition, NaCl was detected with XRD. However, as seen in Fig. 14, the episode of high Cl and Na content did not happen during the second winter despite similar weather conditions. Therefore, the road salt treatment should not be assumed to explain the anomalously high Cl and Na contents. Furthermore, the seasonal evolution of the rest of elements was also studied. Figure 15 shows the evolution of Fe, Si and Al, as an example. As can be observed, no seasonal trend has been found since no composition is repeated between similar months or seasons. However, the seasonal study reveals interesting correlations between elements. As observed in Fig. 14, Cl and Na show similar trends. Likewise, clear relationships between Fe, Si and Al can be observed (Fig. 15). Figure 16 shows the best correlation between elements. Left panels (a) show the

**Fig. 10** X-ray diffractogram of fly ash (the peak marked as Sy\* belongs to the November 1st diffractogram)

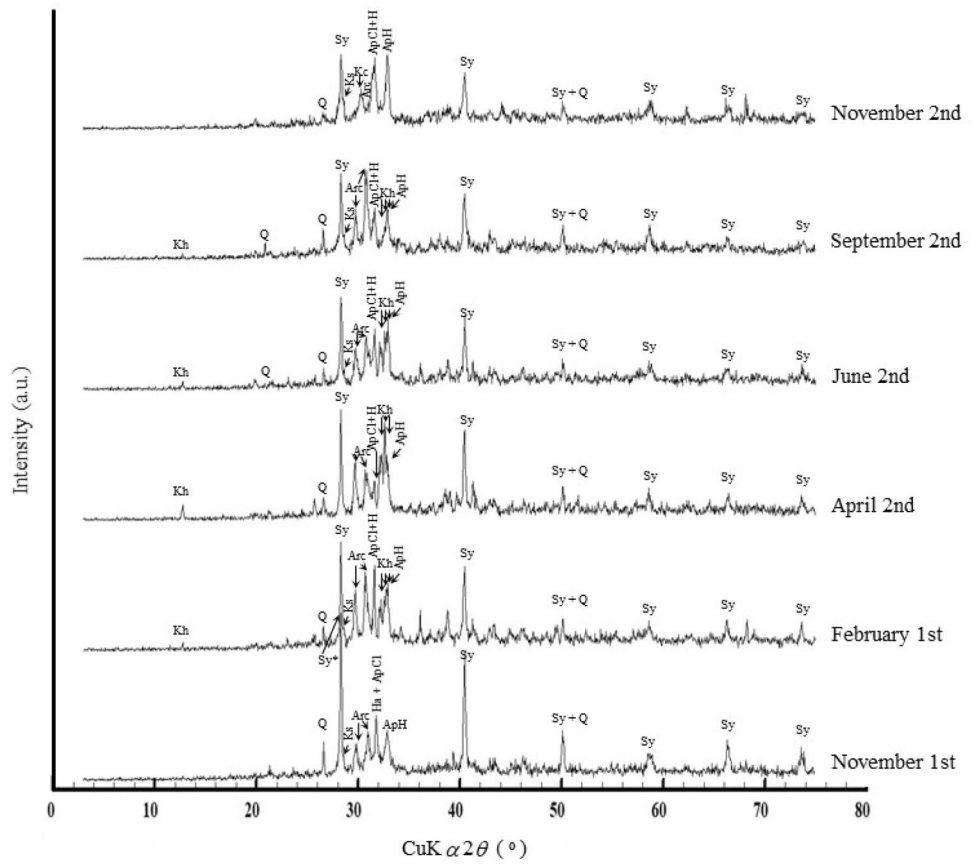


**Fig. 11** X-ray diffractogram of bottom ash. (the peak marked as Q\* belongs to the April 2nd diffractogram)

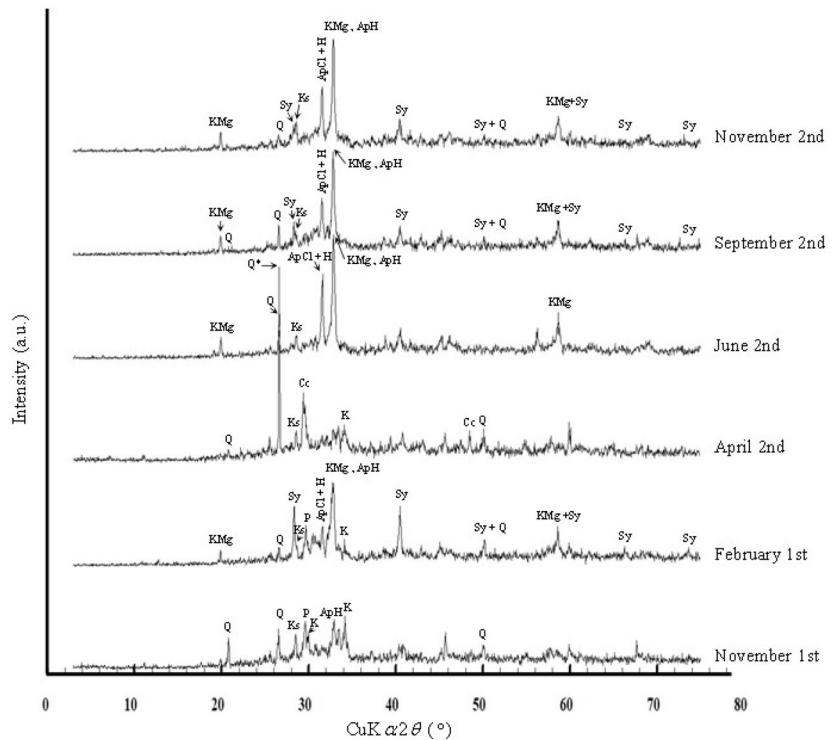


**Fig. 12** X-ray diffractogram of laboratory, fly and bottom ash of June 2nd. Original ash and their insoluble fractions, obtained after water washing

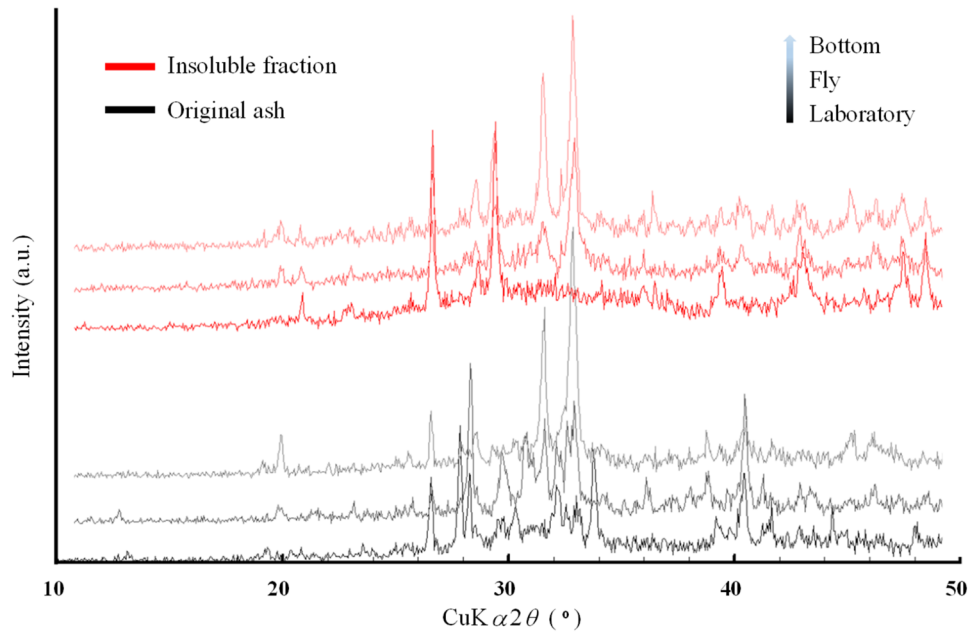


**Fig. 13** Peak height of the highest peak of KCl along months

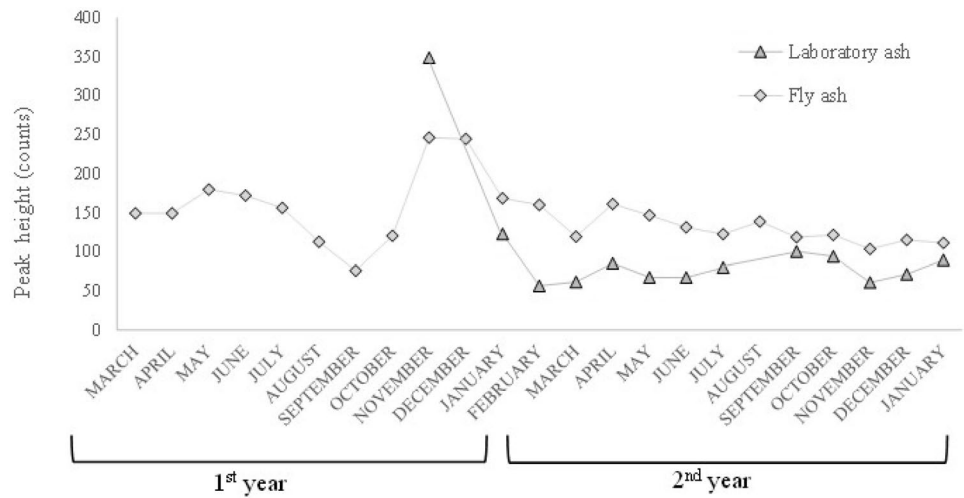


**Fig. 14** Fly ash seasonal evolution for Cl and Na

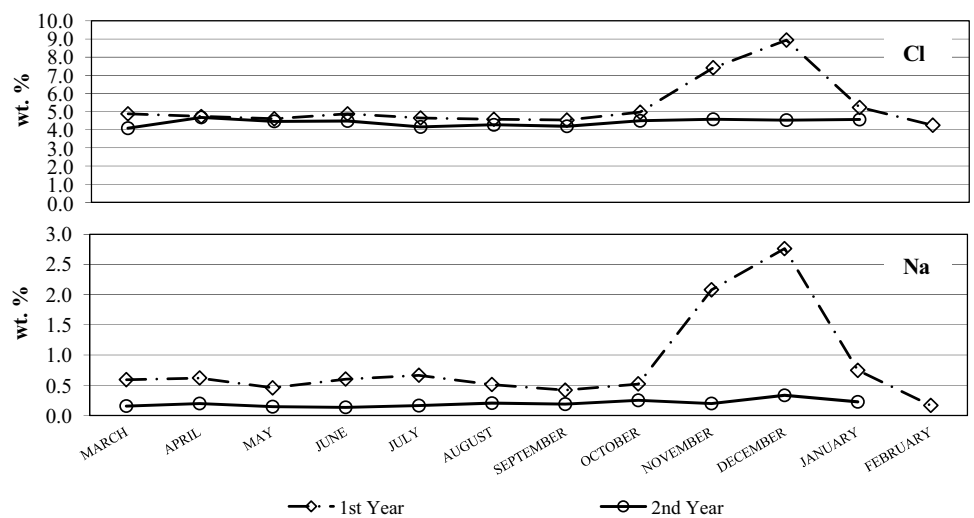
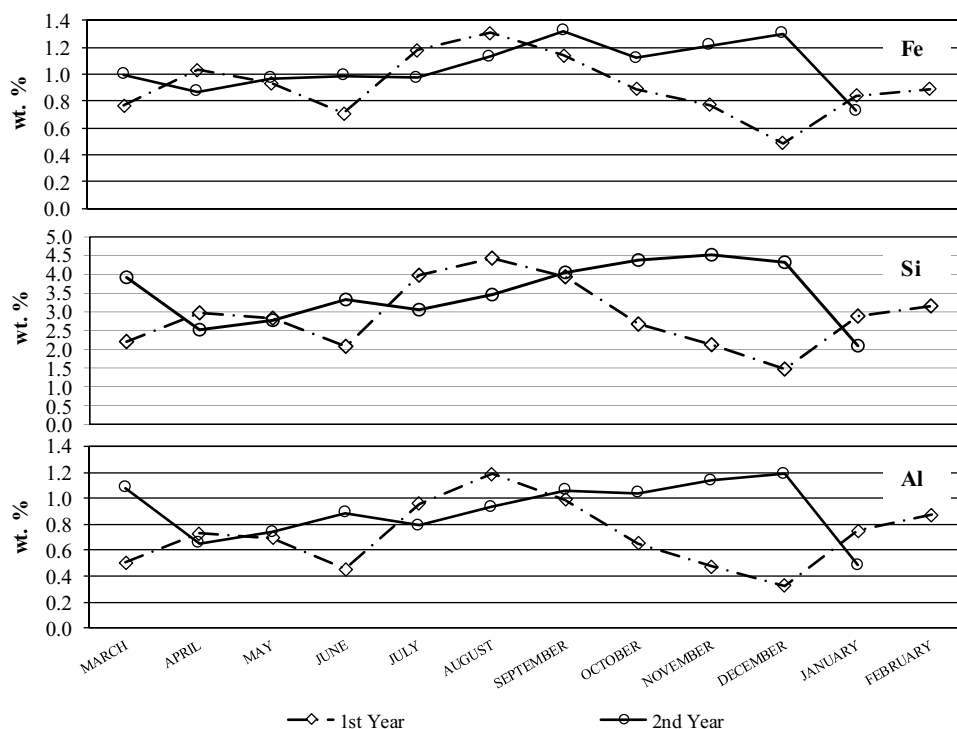


**Fig. 15** Fly ash seasonal evolution for Fe, Si and Al



correlations considering November (1st year) and December (1st year) and the right panels (b) show the same correlations discarding these months. This distinction was done to show that the correlation between Cl and Na ( $R^2=0.98$  for laboratory ash and  $0.96$  for fly ash) is much better when considering November and December 1st year (a). On the contrary, this correlation is very weak ( $R^2=0.41$  for laboratory ash and  $0.64$  for fly ash) when these months were not considered (b), meaning that there is no significant correlation between these two elements when the usual untainted feedstocks are used, and thus adding consistency to the attributed contamination with NaCl during the aforementioned months. Nevertheless, the strong relationship between Si, Al and Fe ( $R^2=0.8$ – $0.9$  for laboratory ash) is clear in the two scenarios (including and discarding November and December 1st year). This correlation suggests a common origin for most of the content of these elements. As an indicative value, the average Al content on biomass basis for the samples measured in this study is 1754 ppm, which is very high for a fruit-based biomass, and could be derived from soil contamination [37]. In fact, Si, Al and Fe are usually present in high quantities in soil. This contamination could be derived from storage, handling and transport operations, and at the studied plant, during the milling pretreatment, stones in the feedstock are always observed. Nevertheless, this probable contamination has never led to troublesome deposit formation on the superheaters.

## Ash Applications

Reuse and recycling of biomass ash as a new resource can enhance the development of a circular and sustainable economy. Knowing the quality of recovery ash, including its variability, is necessary to efficiently look for applications [38]. Therefore, this study provides information about the chemical and mineralogical composition and the variability of fly and bottom ash from orujillo. This information is useful to establish the ash quality control, the possible ash applications, and the ash pretreatment (removal of unburnt carbon, thermal treatment, blending with other kind of ash...) needed to adapt it for its final use.

Considering the low acid “K” type classification [18] of the recovery ash obtained at the studied plant (Fig. 8), a wide variety of utilization possibilities can be foreseen. Some of these possible uses are: fluxing materials, detergents, activate carbons, recovery of water-soluble major, minor and trace elements, glass and glass ceramics, fertilization, insulators and others [39].

Some of the aforementioned applications are already being carried out or are under study. Ash from orujillo has been widely used as fertilizer because of its high potassium content [40]. In fact, fly ash from the studied plant has been usually sold to fertilizer companies. Other possible uses for this recovery ash are the manufacture



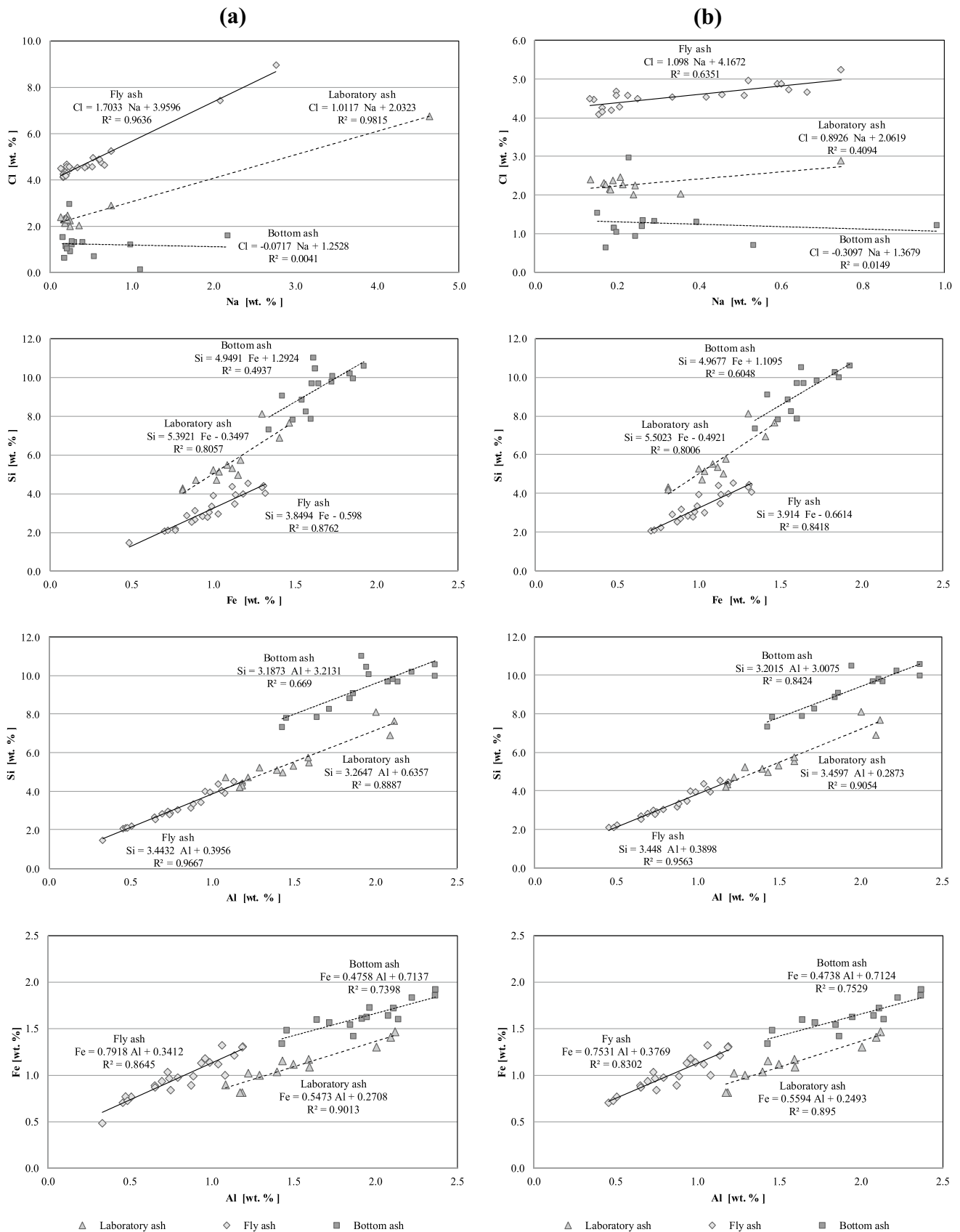


**Fig. 16** Correlation between elements in laboratory, fly and bottom ash. **a** Considering all samples **b** Discarding November and December 1st year

of construction materials. Fly and bottom ash are characterized by two properties with high impact when used in ceramic applications. They have a high content of fluxing oxides ( $K_2O$ ) and auxiliary fluxing oxides ( $CaO$  and  $MgO$ ), both summing up to 52% wt. for both fly and bottom ash, which could reduce the firing temperature of ceramic products by lowering their melting point. Another property that distinguishes the studied ash is its high LOI content, achieving 23.6% wt. and 14.7% wt. for fly and bottom ash, respectively (Fig. 7). LOI content represents unburned carbon, water that volatilizes from moisture and hydrated phases, and  $CO_2$  from carbonate decomposition (Table 4). These compounds volatilize at the ceramic firing temperatures and can form pores in the ceramic products, which improves the thermal insulation [25]. Such characteristics would allow the production of eco-friendly bricks, whose sustainability would be based on both the use of wastes (ash), up to 10% [41], to 20% [25] or to 25% [24], and the energy and  $CO_2$  reduction derived from a lower fuel consumption in ceramic furnaces, due to the decrease in the ceramic melting point, as recently proved [41].

Another interesting application of orujillo ash [42, 43], as well as of other kind of biomass ash [44, 45], is the use as adsorbent to remove metal ions from aqueous solutions. Furthermore, the studied ash is strongly alkaline due its high  $K_2O/Na_2O$  or  $CaO$  content (Fig. 7) and this characteristic makes it useful in acidic industrial wastewaters treatment processes [42].

It must be noticed that using ash with abnormal composition would require revising the proportions to be employed for typical ash. For example, the contamination shown in this study ( $Cl$  and  $Na$ ) produces ash with an abnormally high content of sodium and  $KCl$  which significantly decrease their characteristic melting points [46] and thus, could decrease more than expected the paste sintering point in clay or ceramic bodies. Furthermore, high  $KCl$  is expected to cause scumming [47], and an excess of chlorine could cause harmful corrosion on the industrial furnace metal elements. Moreover, if used in the production of concrete, an excess in chlorine content could attack the oxide passivation layer of concrete, causing a negative effect on the durability and strength of concrete [48]. All these undesirable effects demonstrate the necessity to control both the fed orujillo and the derived ash, especially the  $Cl$  and  $Na$  contents, at the power plant and at the facility for ash recycling, respectively.

## Conclusion

A complete characterization of feedstock, bottom and fly ash collected along more than a year in a 16 MW orujillo's suspension-fired boiler power plant has been made. One of the main highpoints of this study is the characterization of

ash from a real biomass boiler instead of, as usual in most of the works dealing with biomass combustion, ash obtained under well-controlled laboratory conditions.

The study is focused on the distribution of elements and crystalline phases between fly and bottom ash and, on the possible feedstock's contamination and its implications. The following conclusions can be drawn:

- (1) Composition of feedstock is quite invariable except when some contamination occurs. Along more than a year, a clear contamination with  $Cl$  and  $Na$  has been observed in two-month samples (weight contents 2.5 and 18 times higher than usually, respectively) and a clear correlation between the increase in  $Cl$  and  $Na$  shows a common origin. Furthermore, the identification of  $NaCl$  with XRD, suggest possible salt contamination. The seasonal study proves that salt road treatment is not the contamination source since this contamination is not related to the winter conditions. Other possible sources of contamination with  $Na$  and  $Cl$  are the use of table olives or the spilling of any other sodium- and chlorine-rich substance on the feedstock. However, no specific contamination source could be proved.
- (2) No seasonal trend has been found, since no composition is repeated between similar months or seasons.
- (3) Fly ash enrichment in volatile species ( $K$ ,  $Cl$ ,  $S$ ) has been evidenced, as well as the enrichment in  $Si$ ,  $Al$ ,  $Fe$ ,  $Ca$  and  $P$  in bottom ash. It is remarkable that fly ash potassium enrichment is very high, and it is even higher than the one observed in straw fly ash by other authors.
- (4) The main component of fly ash is potassium (~40% wt as  $K_2O$ ), four times higher than the second one which is calcium. Other important components are silicon (~7% wt as  $SiO_2$ ), sulfur (~6% wt as  $SO_3$ ) and chlorine (~4.5% wt). This shows that  $KCl$ ,  $K_2SO_4$  and potassium carbonates are distinctive of this ash.
- (5) The main component of bottom ash is potassium (~30% wt as  $K_2O$ ) followed by silicon (~20% wt as  $SiO_2$ ) and calcium (~18% wt. as  $CaO$ ). The prominent crystalline phases of this ash are phosphates, silicates and carbonates of calcium and magnesium, rather than potassium carbonates.
- (6) Due to its composition, fly ash is adequate to be used as fertilizer component and as component for construction materials. Its potassium content is interesting for many applications (such as alkali activator) but when  $Na$  and  $Cl$  contamination occurs the high and unexpected contents could cause some troubles. For instance, they could decrease the strength of concrete or the paste melting point in ceramic bodies.
- (7) The feedstock's aluminum content, 1754 ppm, (higher than expected for a biomass source) and the clear cor-

relation between Fe, Al and Si contents suggest the presence of soil contamination, although this has not resulted in troublesome deposit formation.

- (8) A relationship between high Cl and Na contents and a harmful deposit growth has been observed. Therefore, Cl and Na contents should be included in the plant feedstock's quality control when orujillo is used.

**Supplementary Information** The online version contains supplementary material available at <https://doi.org/10.1007/s12649-021-01609-5>.

**Acknowledgements** The company Energías de la Mancha, S.A. is gratefully acknowledged for his great implication on this study participating on the biomass and ash sampling as well as providing all required information about the plant operation. The Government of Castilla-La Mancha (Spain) is also acknowledged for their financial support through the BIOENTE Research Project (Reference SBPLY/19/180501/000283). The authors would like to thank the University of Castilla-La Mancha (UCLM) for financing Esperanza Monedero through the Call for access to the Spanish System for Science, Technology and Innovation (UCLM's Own Research Plan), funded by the European Social Fund.

**Funding** Open Access funding provided thanks to the CRUE-CSIC agreement with Springer Nature.

## Declarations

**Conflict of interest** The authors declare that they have no conflict of interest.

**Open Access** This article is licensed under a Creative Commons Attribution 4.0 International License, which permits use, sharing, adaptation, distribution and reproduction in any medium or format, as long as you give appropriate credit to the original author(s) and the source, provide a link to the Creative Commons licence, and indicate if changes were made. The images or other third party material in this article are included in the article's Creative Commons licence, unless indicated otherwise in a credit line to the material. If material is not included in the article's Creative Commons licence and your intended use is not permitted by statutory regulation or exceeds the permitted use, you will need to obtain permission directly from the copyright holder. To view a copy of this licence, visit <http://creativecommons.org/licenses/by/4.0/>.

## References

- Bashir, M.S., Jensen, P.A., Frandsen, F.J., Wedel, S., Dam-Johansen, K., Wadenbäck, J., Pedersen, S.T.: Ash transformation and deposit build-up during biomass suspension and grate firing: full-scale experimental studies. *Fuel Process. Technol.* **97**, 93–106 (2012)
- Hansen, S.B., Jensen, P.A., Frandsen, F.J., Wu, H., Bashir, M.S., Wadenbäck, J., Sander, B., Glarborg, P.: Deposit probe measurements in large biomass-fired grate boilers and pulverized-fuel boilers. *Energy Fuels* **28**, 3539–3555 (2014)
- Obernberger, I., Biedermann, F., Widmann, W., Riedl, R.: Concentrations of inorganic elements in biomass fuels and recovery in the different ash fractions. *Biomass Bioenergy* **12**(3), 211–224 (1997)
- Michelsen, H.P., Frandsen, F., Dam-Johansen, K., Larsen, O.H.: Deposition and high temperature corrosion in a 10 MW straw fired boiler. *Fuel Process. Technol.* **54**, 95–108 (1998)
- Hansen, S.B., Jensen, P.A., Jappe Frandsen, F., Wu, H., Sander, B., Wadenbäck, J., Glarborg, P.: Deposit probe measurements in Danish grate and pulverized fuel biomass power boilers. In *Proceedings. Impacts of fuel quality on power production and the environment*. Puchberg, Austria (2012)
- Lanzerstorfer, C.: Grate-fired biomass combustion plants using forest residues as fuel: enrichment factors for components in the fly ash. *Waste Biomass Valor.* **8**, 235–240 (2017)
- Nordgren, D., Hedman, H., Padban, N., Boström, D., Öhman, M.: Ash transformations in pulverised fuel co-combustion of straw and woody biomass. *Fuel Process. Technol.* **105**, 52–58 (2013)
- Andalusian Energy Agency: La bioenergía en Andalucía (In Spanish). <https://www.agenciaandaluzadelaenergia.es/es/biblioteca/la-bioenergia-en-andalucia> (2020). Accessed May 2021
- Williams, O., Eastwick, C., Kingman, S., Giddings, D., Lormor, S., Lester, E.: Overcoming the caking phenomenon in olive mill wastes. *Ind. Crops Prod.* **101**, 92–102 (2017)
- Perry, M., Rosillo-Calle, F.: Country report for United Kingdom. Report T40UK5/09. International Energy Agency, Bioenergy <https://task40.ieabioenergy.com/wp-content/uploads/sites/6/2013/09/iea-task-40-country-report-2009-uk.pdf> (2009). Accessed May 2021
- Perry, M., Rosillo-Calle, F.: Co-firing report-United Kingdom. Report T40UK02R International Energy Agency, Bioenergy (2006)
- European Committee for Standardization: EN ISO 17225–1:2014. Solid biofuels. Fuel specifications and classes. Part 1: General requirements. Brussels, Belgium (2014)
- Mlonka-Mędrala, A., Magdziarz, A., Gajek, M., Nowińska, K.: Alkali metals association in biomass and their impact on ash melting behaviour. *Fuel* **261**, 116421 (2020)
- Jin, X., Ye, J., Deng, L., Che, D.: Condensation behaviors of potassium during biomass combustion. *Energy Fuels* **31**, 2951–2958 (2017)
- Capablo, J.: Formation of alkali salt deposits in biomass combustion. *Fuel Process. Technol.* **153**, 58–73 (2016)
- Febrero, L., Granada, E., Regueiro, A., Míguez, J.L.: Influence of combustion parameters on fouling composition after wood pellet burning in a lab-scale low-power boiler. *Energies* **8**, 9794–9816 (2015)
- Shao, Y., Wang, J., Preto, F., Zhu, J., Xu, C.: Ash deposition in biomass combustion or co-firing for power/heat generation. *Energies* **5**, 5171–5189 (2012)
- Vassilev, S.V., Baxter, D., Andersen, L.K., Vassileva, C.G.: An overview of the chemical composition of biomass. *Fuel* **89**(5), 913–933 (2010)
- Sánchez, A.H., García, P., Rejano, L.: Elaboration of table olives. *Int. J. Fats Oils* **57**(1), 86–94 (2006)
- López, A., García, P., Garrido, A.: Multivariate characterization of table olives according to their mineral nutrient composition. *Food Chem.* **106**, 369–378 (2008)
- Lapuerta, M., Acosta, A., Pazo, A.: Fouling deposits from residual biomass with high sodium content in power plants. *Energy Fuels* **29**, 5007–5017 (2015)
- Fuller, A., Stegmaier, M., Schulz, N., Menke, M., Schellhorn, H., Knödler, F., Maier, J., Scheffknecht, G.: Use of wood dust fly ash from an industrial pulverized fuel facility for rendering. *Constr. Build. Mater.* **189**, 825–848 (2018)
- Skrifvars, B.J., Laurén, T., Hupa, M., Korbee, R., Ljung, P.: Ash behaviour in a pulverized wood fired boiler—a case study. *Fuel* **83**, 1371–1379 (2004)

24. Bonet-Martinez, E., Pérez-Villarejo, L., Eliche-Quesada, D., Sánchez-Soto, P.J., Carrasco-Hurtado, B., Castro-Galiano, E.: Manufacture of sustainable clay ceramic composite with composition  $\text{SiO}_2\text{-Al}_2\text{O}_3\text{-CaO-K}_2\text{O}$  materials valuing biomass ash from olive pomace. *Mater. Lett.* **229**, 21–25 (2018)
25. Eliche-Quesada, D., Leite-Costa, J.: Use of bottom ash from olive pomace combustion in the production of eco-friendly fired clay bricks. *Waste Manage.* **48**, 323–333 (2016)
26. Hernández, J.J., Lapuerta, M., Monedero, E., Pazo, A.: Biomass quality control in power plants: technical and economical implications. *Renewable Energy* **115**, 908–916 (2018)
27. Nergiz, C., Engez, Y.: Compositional variation of olive fruit during ripening. *Food Chem.* **69**, 55–59 (2000)
28. Spanish Association for Standardisation (AENOR): UNE 164003. Biocombustibles sólidos. Especificaciones y clases de biocombustibles. Huesos de aceituna (In Spanish) Spain, Madrid (2014)
29. Zajac, G., Szyszlak-Bargłowicz, J., Gołębowski, W., Szczepanik, M.: Chemical characteristics of biomass ashes. *Energies* **11**, 2885 (2018)
30. Hupa, M.: Ash-related issues in fluidized-bed combustion of biomasses: recent research highlights. *Energy Fuels* **6**(2), 4–14 (2012)
31. Shah, K.V., Cieplik, M.K., Bertrand, C.I., Van de Kamp, W.L., Vuthaluru, H.B.: Correlating the effects of ash elements and their association in the fuel matrix with the ash release during pulverized fuel combustion. *Fuel Process. Technol.* **91**, 531–545 (2010)
32. Caponio, F., Squeo, G., Difonzo, G., Pasqualone, A., Summo, C., Paradiso, V.M.: Has the use of talc an effect on yield and extra virgin olive oil quality? *J. Sci. Food Agric.* **96**, 3292–3299 (2016)
33. Vassilev, S.V., Baxter, D., Vassileva, C.G.: An overview of the behaviour of biomass during combustion: Part I. Phase-mineral transformations of organic and inorganic matter. *Fuel* **112**, 391–449 (2013)
34. Johansen, J.M., Jakobsen, J.G., Frandsen, F.J., Glarborg, P.: Release of K, Cl, and S during pyrolysis and combustion of high-chlorine biomass. *Energy Fuels* **25**, 4961–4971 (2011)
35. Niu, Y., Zhu, Y., Tan, H., Wang, X., Hui, S., Du, W.: Experimental study on the coexistent dual slagging in biomass-fired furnaces: alkali- and silicate melt-induced slagging. *Proc. Combust. Inst.* **35**, 2405–2413 (2015)
36. Niu, Y., Tan, H., Hui, S.: Ash-related issues during biomass combustion: alkali-induced slagging, silicate melt-induced slagging (ash fusion), agglomeration, corrosion, ash utilization, and related countermeasures. *Prog. Energy Combust. Sci.* **52**, 1–61 (2016)
37. Cherney, J.H., Ketterings, Q., Cherney, D.J.R.: Soil contamination of grass biomass hay: measurements and implications. *Bioenerg. Res.* **9**, 773–781 (2016)
38. Gupta, V., Pathak, D.K., Siddique, S., Kumar, R., Chaudhary, S.: Study on the mineral phase characteristics of various Indian biomass and coal fly ash for its use in masonry construction products. *Constr. Build. Mater.* **235**, 117413 (2020)
39. Vassilev, S., Baxter, D., Andersen, L.K., Vassileva, C.G.: An overview of the composition and application of biomass ash. Part 2. Potential utilisation, technological and ecological advantages and challenges. *Fuel* **105**, 19–39 (2013)
40. Valta, K., Aggeli, E., Papadaskalopoulou, C., Panaretou, V., Sotiropoulou, A., Malamis, D., Moustakas, K., Haralambous, K.J.: Adding value to olive oil production through waste and wastewater treatment and valorisation: the case of Greece. *Waste Biomass Valor* **6**, 913–925 (2015)
41. Monedero, E., Hernández, J.J., Collado, R., Pazo, A., Aineto, M., Acosta, A.: Evaluation of ashes from agro-industrial biomass as a component for producing construction materials. *J. Cleaner Production* **318**, 128517 (2021)
42. Bouzid, J., Elouear, Z., Ksibi, M., Feki, M., Montiel, A.: A study on removal characteristics of copper from aqueous solution by sewage sludge and pomace ashes. *J. Hazard. Mater.* **152**, 838–845 (2008)
43. Elouear, Z., Bouzid, J., Boujelben, N., Feki, M., Montiel, A.: The use of exhausted olive cake ash (EOCA) as a low cost adsorbent for the removal of toxic metal ions from aqueous solutions. *Fuel* **87**, 2582–2589 (2008)
44. Rodríguez-Díaz, J.M., Prieto, J.O., Bravo, L.R., da Silva, M.G.C., da Silva, V.L., Arteaga-Pérez, L.E.: Comprehensive characterization of sugarcane bagasse ash for its use as an adsorbent. *Bioenerg. Res.* **8**, 1885–1895 (2015)
45. Barbosa, R., Lapa, N., Lopes, H., Günther, A., Dias, D., Mendes, B.: Biomass fly ashes as low-cost chemical agents for Pb removal from synthetic and industrial wastewaters. *J. Colloid Interface Sci.* **424**, 27–36 (2014)
46. Niu, Y., Lv, Y., Zhang, X., Wang, D., Li, P., Hui, S.: Effects of water leaching (simulated rainfall) and additives (KOH, KCl, and  $\text{SiO}_2$ ) on the ash fusion characteristics of corn straw. *Appl. Therm. Eng.* **154**, 485–492 (2019)
47. De la Casa, J.A., Castro, E.: Recycling of washed olive pomace ash for fired clay brick manufacturing. *Constr. Build. Mater.* **61**, 320–326 (2014)
48. Hinojosa, M.J.R., Galvin, A.P., Agrela, F., Perianes, M., Barbudo, A.: Potential use of biomass bottom ash as alternative construction material: conflictive chemical parameters according to technical regulations. *Fuel* **128**, 248–259 (2014)

**Publisher's Note** Springer Nature remains neutral with regard to jurisdictional claims in published maps and institutional affiliations.

## Authors and Affiliations

Amparo Pazo<sup>1</sup>  · Magin Lapuerta<sup>2</sup>  · Anselmo Acosta<sup>3</sup>  · Juan J. Hernández<sup>2</sup>  · Esperanza Monedero<sup>1</sup> 

<sup>1</sup> Instituto de Investigación en Energías Renovables, University of Castilla-La Mancha, 02006 Albacete, Spain

<sup>2</sup> Escuela Técnica Superior de Ingeniería Industrial, University of Castilla-La-Mancha, Avda, Camilo José Cela s/n, 13071 Ciudad Real, Spain

<sup>3</sup> Facultad de Ciencias y Tecnologías Químicas, University of Castilla-La-Mancha, Avda, Camilo José Cela s/n, 13071 Ciudad Real, Spain